Application of information technologies for automation of metallurgical melts surface properties calculations

Tetiana Levytska[1][0000-0003-3359-1313]

[1]Priazovsky State Technical University, Universytets'ka str.7, Mariupol 87555, Ukraine
tlevitiisys@gmail.com

Abstract. An experimental facility has been developed for researching the surface properties of metallurgical melts, which, unlike the known ones, is equipped with an optical system and a PC, that allow a digital image of a lying drop, obtained in the experiment, to be processed using a high-speed software package, which significantly reduces the time of the experiment, allows to store data and simplifies the work of the experimenter.

Keywords: surface properties, physico-chemical experiment, experimental facility, digital image, computer, segmentation, recognition, linear filtering, pixel, intensity levels

1 Introduction

The laborious and expensive high-temperature physicochemical measurements are characterized by a change in the studying object during the experiment due to the interaction with the structural materials of the measuring cell and the furnace atmosphere [1]. Therefore, it is very important to reduce the duration of the experiment, to measure the maximum possible number of properties during this time and to strive to automate the work of the experimenter [2-3]. With the advent of digital technology for recording measurement information and processors for its processing, such a task becomes real.

The high speed and accuracy of digital recorders allow multiple measurements of each characteristic in a period of time until they change, which reduces systematic error and makes it possible to effectively apply statistical methods to reduce random error [4-5]. Naturally, the transition to digital technology and partial automation of the experiment should be accompanied by appropriate changes in the calculation methods and approaches to their implementation.

Recently, more attention has been paid to methods based on the analysis of a digitized image of a two- and three-phase contact zone during an experimental research of both surface and interfacial tension, and contact angles. Obviously, the further development of the fixed-drop method is directly related to the development of new methods and specially developed algorithms that allow automatic computer calculation of surface properties. To date, there are no well-tested, modern, high-

precision, experimental methods for measuring surface and interfacial tension, therefore the development of this direction is relevant and promising.

2 Formal problem statement

It is known [6] that the contour of a drop is defined by the Laplace's equation of a capillary and it has to be written like the differential second-order equation:

$$\frac{y''}{\left[1+(y')^2\right]^{\frac{3}{2}}}+\frac{y'}{x\left[1+(y')^2\right]^{\frac{1}{2}}}=\frac{(y+y_0)(\rho_1-\rho_2)\cdot g}{\sigma}, \quad (1)$$

where
σ – surface tension, N/m^2;
ρ_2 –density of the medium, where the drop is, kg/m^3;
ρ_1 –density of the medium, which is form the drop, kg/m^3;
g – acceleration of gravity, m/s^2;
y – coordinate of the point on the surface along the vertical axis;
y_0 – coordinate of the point on the top along the vertical axis.

3 Literature review

There are different methods of the experimental definition the surface tension of liquids: method of capillary rise, ring or slab detachment method, method of a recumbent drop, method of a hanging drop, drop weight method, method of the maximum pressure in gas bubble. Method of a recumbent drop gives the most exact result and nowadays it is widely used in the high-temperature searches [7-8].

In this method the metal drop melts on the horizontal refractory substrate or forcibly formed under the sharp edge of the crucible. Drop are photographed at a temperature of shaping and then it is measured to know its maximum diameter ($2r$) and inches under it (h).

All known methods described in the literature [6-20] are based on the use of the system parameters connection with some characteristic dimensions of the experimental drop profile. According to the tables with theoretical droplet shapes that have been calculated in advance, the connection between the characteristic sizes and the droplet parameters are made, or using the formulas that approximate the table values, the system parameters are found.

However, the calculation of capillary characteristics using tables is inconvenient and time consuming. It is not possible to fully automate such a calculation.

The inconvenience associated with the tabular description of the function led S.I. Popel, Y.P. Nikitin and S.M. Ivanov to the graphical integration of the equation [17]. The accuracy of the graphs published by them is 2–3%. The method presented by them is applicable to drops of arbitrary size. The calculation is carried out by the

experimenter manually. The method of graphical integration gives results that are close enough to those obtained by Bashfort and Adams, who calculated them in a more accurate way [7]. Manual construction of graphs for calculating σ is a complex and lengthy process, it is not possible to improve the accuracy of the method and make any changes to those already published by S.I. Poppel and other graphs. The method of calculation proposed in the thesis allowed us to significantly speed up data processing and to fully automate the calculation of the surface tension of melts with a high degree of accuracy (less than 0.5%) compared to known methods.

Photographic methods of image registration, which are traditionally used in the practice of studying the capillary properties of melts according to the shape of a lying drop, don't allow obtaining final results directly in the course of the experiment. The tasks that confront the experimenter in this case — the processing of photographic materials, the manual measurement of photographs and the calculation of capillary characteristics using tables are very laborious and time consuming. Inevitably, by measuring the image, and especially by carrying out a tangent, the researcher introduces elements of subjectivity into this procedure, and the measurement error depends on the quality of the image. For example, tracing the maximum diameter per eye can give an initial error of 1.5%.

Analysis of the digitized image of the zone of two-and three-phase contact allows you to fully automate the calculations. Most of the known measurement methods are done manually. Although some automated systems using cameras [9] and cameras on a CCD matrix [8] are described. A number of calculation algorithms have been developed [9-11]. According to the authors of the article [12-13], such systems have not received wide distribution, and now further research is needed on methods, algorithms and systems for measuring capillary properties. The raster image of a large drop is formed using a digital camera[14]. The direct digital image is then processed on a PC. In this work, the Dorsey method is used. Most of the known measurement methods are done manually. Although some automated systems using cameras [7] and cameras on a CCD matrix [8] are described. A number of calculation algorithms have been developed [9-11]. According to the authors of the article [12-13], such systems have not received wide distribution, and now further research is needed on methods, algorithms and systems for measuring capillary properties. The raster image of a large drop is formed using a digital camera[14]. The direct digital image is then processed on a PC. In this work, the Dorsey method is used.

The analytic solution this differential equation doesn't have. An approximate solution can be obtained with a predetermined degree of accuracy. All known techniques described in the literature [15-19] are based on using of the coupling of the system parameters with certain characteristic dimensions of the experimental drop profile. According to the sheets with theoretical drop shapes, which are calculated in advance, a connection is made between the characteristic dimensions and parameters of the drop, or by the formulas approximating the tabulated values, find the parameters of the system. Calculating the capillary characteristics by using tables is inconvenient and time-consuming.

An analysis of the theoretical aspects of the recumbent drop method has shown that the previously developed formulas and tables are either difficult to apply or not

applicable at all for PC calculations, which requires transformations of the Laplace's equation to a form convenient for computer mathematical processing.

4 The numerical solution of the Laplace differential equation by empirical formulas

To find the particular solutions of the differential equation (1) that satisfies the initial conditions $y(0) = 0\,;\, y'(0) = 0$ for different values of the capillary constant, let's use the geometric meaning of the first and second derivatives.

As a result, was obtained the expression:

$$\frac{y''}{\left[1 + (y')^2\right]^{3/2}} = \frac{1}{R}, \tag{2}$$

which determines the plane curvature of the curve and the first derivative is equal to the tangent of the angle of inclination of the tangent to the axis 0x. Substituting these values into equation (1), was introduced the substitution:

$$A = \frac{\sigma}{(\rho_1 - \rho_2) \cdot g}. \tag{3}$$

So it was observed:

$$\frac{1}{R} + \frac{tg\varphi}{x \cdot \dfrac{1}{cos\varphi}} = \frac{y + y_o}{A}, \tag{4}$$

$$\frac{tg\varphi}{x \cdot \dfrac{1}{\cos\varphi}} = \frac{\sin\varphi \cdot \cos\varphi}{x \cdot \cos\varphi}, \tag{5}$$

$$R = \frac{A}{(y - y_0) - A \cdot \dfrac{\sin\varphi}{x}}. \tag{6}$$

Equation (6) defines the radius of curvature at any point of the meridian section of the drop, but contains an undefined ratio (sin φ)/x. When approaching the top of the drop of $x \to 0$, $y \to 0$, $\varphi \to 0$, the vertex both main droplet radius R_1 and R_2 drops of curvature equal to each other and equal to R_0. From the Laplace's equation (1) for this case was observed

$$R_0 = \frac{2A}{y_0}.$$

Having $R_1 \to R_2 \to R_0 = 2 \cdot A/y_0$, this was substituted into equation (2) and found the limit of the right side of the resulting expression.

$$\frac{2\cdot A}{y_0}=\lim_{x\to 0}\frac{A}{(y+y_0)-A\cdot\sin\varphi/x}=\frac{A}{y_0-A\cdot\lim\limits_{x\to 0}\dfrac{\sin\varphi}{x}}, \tag{7}$$

$$\lim_{x\to 0}\frac{\sin\varphi}{x}=\frac{y_o}{2\cdot A}. \tag{8}$$

Were chosen on the meridional section line three sufficiently close to each other points M_{i-1}, M_i and M_{i+1} and drawn through them the normal lines (Fig. 1).

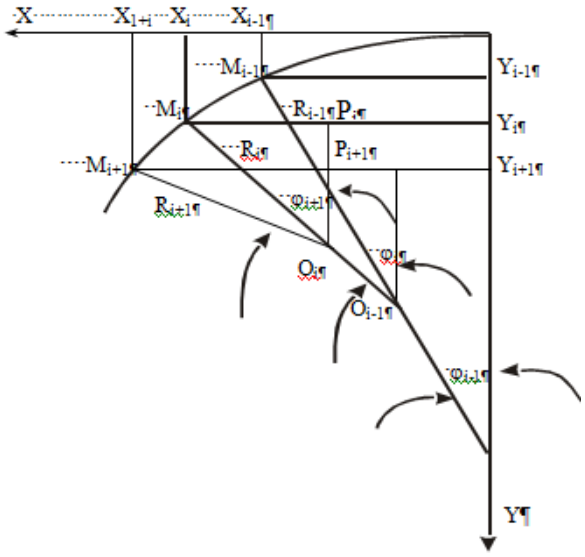

Figure 1. The scheme for constructing the drop elements for numerical integration.

The normal line passing through the point M_{i-1} intersects the normal line passing through the point M_i at the point O_{i-1}, and the normal lines passing through the points M_iM_{i+1} intersect at the point O_i. It was denoted the angles formed by the normal lines $M_{i-1}O_{i-1}$, M_iO_i and $M_{i+1}O_i$, respectively, φ_{i-1}, φ, φ_{i+1}.To numerically integrate the differential equation (1) and calculate the droplet shape, it was assumed that for a sufficiently small change in the current angle φ in the range from φ_{i-1} to φ_i, the radius of curvature R_{i-1} (the segment $M_{i-1}O_{i-1}$ or the segment M_iO_{i-1}) of the initial angle φ_{i-1} of the original abscissa x_{i-1} and the initial ordinate V_{i-1} does not change. In the next interval of variation of the angle φ from φ_i to φ_{i+1}, the radius of curvature R_i (of the segment M_iO_i or $M_{i+1}O_i$) or the other is calculated for a new value of the angle φ_i, the new abscissa x_i and the new ordinate y_i.

From the rectangular triangle $O_iM_{i+1}P_{i+1}$ and $O_iM_iP_i$ was found:

$$\Delta y_i=\left|P_i-P_{i+1}\right|=R_i\cdot\cos\varphi_i-R_i\cdot\cos\varphi_{i+1}=R_i\left[\cos\varphi_i-\cos\varphi_{i+1}\right],$$

$$\Delta x_i = \left|M_{i+1}P_{i+1}\right| - \left|M_iP_i\right| = R_i \cdot \sin\varphi_{i+1} - R_i \cdot \sin\varphi_i = R_i\left[\sin\varphi_{i+1} - \sin\varphi_i\right],$$

$$y_{i+1} = y_i + \Delta y_i$$

$$x_{i+1} = x_i + \Delta x_i .$$

Thus, we have the following algorithm for calculating the meridional section line coordinates of the drop and volume (Fig. 2), which is implemented in the Delphi visual programming system.

We built dependences graphs of the coordinates x = x (φ), y = y (φ) of the meridional section of the drop on the current angle φ, as well as the volume of the part of the drop between its top and plane y = y_0 = const, shown schematically in Fig. 3

The graphs of the dependences of the coordinates x = x (φ), y = y (φ) of the Meridional section of the drop from the current angle φ, and also the volume of the part of the drop between its vertex and the plane y = y_0 = const have functions at the corresponding values of the parameters a_x, b_x, c_x, a_y, b_y, c_y, a_v, b_v, c_v.

$$x = a_x \cdot \varphi^{b_x} \cdot \exp(c_x \cdot \varphi) \tag{9}$$

$$y = a_y \cdot \varphi^{b_y} \cdot \exp(c_y \cdot \varphi) \tag{10}$$

$$V = a_v \cdot \varphi^{b_v} \cdot \exp(c_v \cdot \varphi) \tag{11}$$

Therefore, for the empirical description of the numerical solution of the differential equation of the drop form (1), these dependences [4]. The coefficients of the obtained equations are found by the method of rectifying the obtained graphs and introducing new variables. Was found the ratio of the next to the previous value of any of the coordinates

$$\frac{x_{i+1}}{x_i} = \frac{a_x\varphi_{i+1}^{b_x}\exp(c_x\varphi_{i+1})}{a_x\varphi_i^{b_x}\exp(c_x\varphi_i)} = \left[\frac{\varphi_{i+1}}{\varphi_i}\right]^{b_x} e^{c_x\left[\varphi_{i+1}-\varphi_i\right]} \tag{12}$$

Take the natural logarithms from the left and right sides of this relation:

$$\ln(x_{i+1}/x_i) = b_x \ln(\varphi_{i+1}/\varphi_i) + c_x\left[\varphi_{i+1} - \varphi_i\right] = b_x \ln(\varphi_{i+1}/\varphi_i) + c_x\Delta\varphi$$

Denote $\ln(x_{i+1}/x_i)$ by $\widetilde{x}$, $\ln(\varphi_{i+1}/\varphi_i)$ trough $\tilde{\varphi}$, then was obtained a linear relationship between the variables $\widetilde{x}$ and $\tilde{\varphi}$.

$$\widetilde{x} = b_x \cdot \tilde{\varphi} + c_x \cdot \Delta\varphi \tag{13}$$

While investigation unknown dependencies it is possible random errors associated with the measurement process. To reduce the effect of random measurement errors, was applied the least squares method, which allows to determine the parameters of the

chosen dependence, in which the deviation from the experimental data (in this case, the calculated data) is minimal.

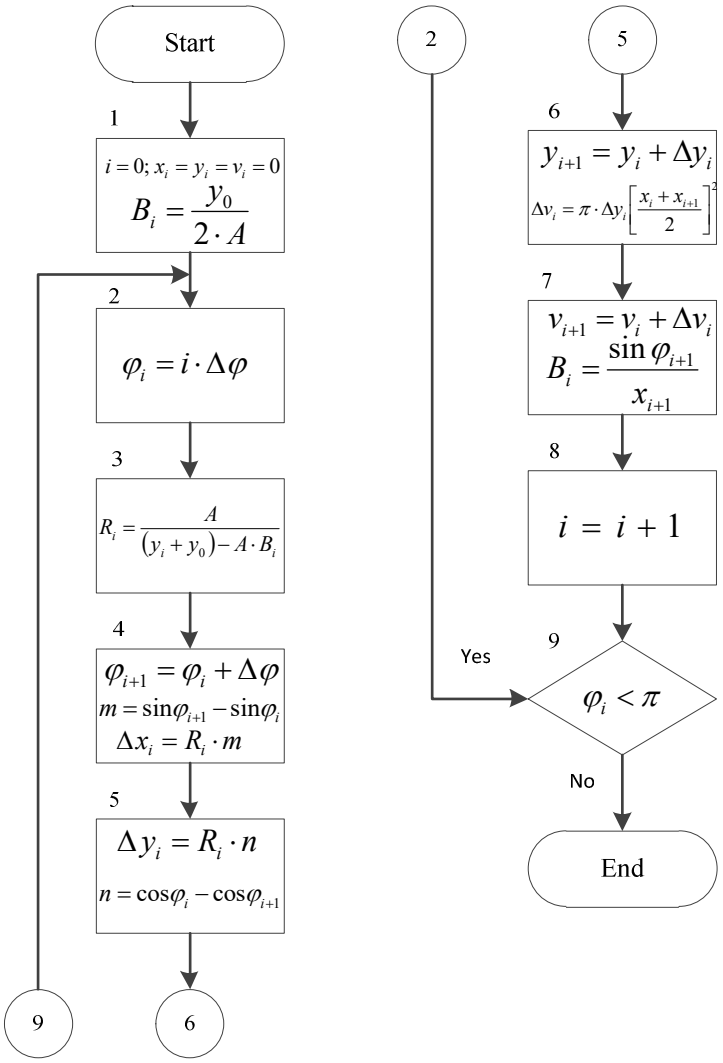

Figure2 .Algorithm for calculating the meridional section line coordinates of the drop and volume

There are calculation results (x_1,φ_1,), (x_2,φ_2),…,(x_n, φ_n) and the form of the function $\widetilde{x} = b_x \cdot \widetilde{\varphi} + c_x \cdot \Delta\varphi$. It is necessary to choose b_x and c_x so that the sum of the squares of the differences between the empirical and calculated values (deviations) is minimal:

$$\Phi(b_x, c_x) = \sum_{i=1}^{n} \varepsilon_i^2 = \sum_{i=1}^{n} [x_i - \widetilde{x}]^2 = \min. \tag{14}$$

When the expression (13) is substituted into condition (14) it was obtained:

$$\Phi(b_x, c_x) = \sum_{i=1}^{n} [b_x \cdot \tilde{\varphi} + c_x \cdot \Delta\varphi - x_i]^2 = \min$$

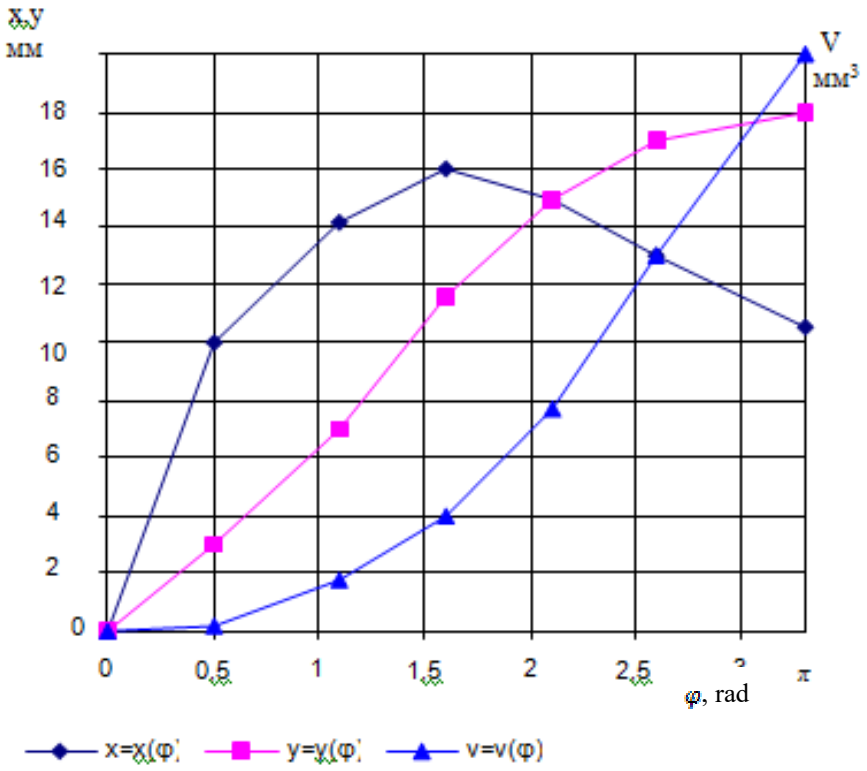

Figure 3. The dependence of the x, y coordinates and the volume of the drop v on the current angle φ

To find the values b_x and c_x that convert the left-hand side of the resulting expression to a minimum, it is necessary to equate the derivatives with respect to zero. A function can have an extremum (min) if all its partial derivatives are zero or nonexistent.

$$\frac{\partial \Phi(b_x, c_x)}{\partial b_x} = 0$$

$$\frac{\partial \Phi(b_x, c_x)}{\partial c_x} = 0$$

$$\begin{cases} 2\sum_{i=1}^{n}[b_x \cdot \widetilde{\varphi} + c_x \cdot \Delta\varphi - x_i] \cdot \widetilde{\varphi} = b_x \cdot \sum_{i=1}^{n}\widetilde{\varphi}^2 + c_x \cdot \sum_{i=1}^{n}\widetilde{\varphi} \cdot \Delta\varphi - \sum_{i=1}^{n}x_i \cdot \widetilde{\varphi} = 0 \\ 2\sum_{i=1}^{n}[b_x \cdot \widetilde{\varphi} + c_x \cdot \Delta\varphi - x_i] \cdot \Delta\varphi = b_x \cdot \sum_{i=1}^{n}\widetilde{\varphi} \cdot \Delta\varphi + c_x \cdot \sum_{i=1}^{n}\Delta\varphi^2 - \sum_{i=1}^{n}x_i \cdot \Delta\widetilde{\varphi} = 0 \end{cases}$$

$$\begin{cases} \underline{\underline{b_x}} \cdot \sum_{i=1}^{n}\widetilde{\varphi}^2 + \underline{c_x} \cdot \Delta\varphi \cdot \sum_{i=1}^{n}\widetilde{\varphi} = \sum_{i=1}^{n}x_i \cdot \widetilde{\varphi} \\ \underline{\underline{b_x}} \cdot \Delta\varphi \cdot \sum_{i=1}^{n}\widetilde{\varphi} + \underline{c_x} \cdot \Delta\varphi^2 \sum_{i=1}^{n}1 = \Delta\widetilde{\varphi} \cdot \sum_{i=1}^{n}x_i \end{cases}$$

This is the final form of the normal least-squares method [5]. It was solved the system and found empirical values according to Cramer's formulas:

$$c_x = \frac{\Delta c_x}{\Delta},$$

$$b_x = \frac{\Delta b_x}{\Delta},$$

$$\Delta = \begin{vmatrix} \sum\varphi^2 & \Delta\varphi\sum_{i=1}^{n}\varphi \\ \Delta\varphi \cdot \sum_{i=1}^{n}\varphi & \Delta\varphi^2 \cdot n \end{vmatrix}, \qquad \Delta_{b_x} = \begin{vmatrix} \sum x_i \cdot \widetilde{\varphi} & \Delta\varphi\sum_{i=1}^{n}\varphi \\ \Delta\varphi \cdot \sum_{i=1}^{n}x_i & \Delta\varphi^2 \cdot n \end{vmatrix},$$

$$\Delta_{c_x} = \begin{vmatrix} \sum\varphi^2 & \sum_{i=1}^{n}x_i \cdot \widetilde{\varphi} \\ \Delta\varphi \cdot \sum_{i=1}^{n}\varphi & \Delta\varphi \cdot \sum_{i=1}^{n}x_i \end{vmatrix},$$

$$b_x = \frac{\Delta b_x}{\Delta} = \frac{\begin{vmatrix} \sum_{i=1}^{n}x_i \cdot \widetilde{\varphi} & \Delta\varphi\sum_{i=1}^{n}\varphi \\ \Delta\varphi \cdot \sum_{i=1}^{n}x & \Delta\varphi^2 \cdot n \end{vmatrix}}{\begin{vmatrix} \sum_{i=1}^{n}\varphi^2 & \Delta\varphi\sum_{i=1}^{n}\varphi \\ \Delta\varphi \cdot \sum_{i=1}^{n}\varphi & \Delta\varphi^2 \cdot n \end{vmatrix}} = \frac{\Delta\varphi^2}{\Delta\varphi^2}\frac{\begin{vmatrix} \sum_{i=1}^{n}x_i \cdot \widetilde{\varphi} & \sum_{i=1}^{n}\varphi \\ \sum_{i=1}^{n}x_i & n \end{vmatrix}}{\begin{vmatrix} \sum_{i=1}^{n}\varphi^2 & \sum_{i=1}^{n}\varphi \\ \sum_{i=1}^{n}\varphi & n \end{vmatrix}} = \frac{\begin{vmatrix} \sum_{i=1}^{n}x_i \cdot \widetilde{\varphi} & \sum_{i=1}^{n}\varphi \\ \sum_{i=1}^{n}x_i & n \end{vmatrix}}{\begin{vmatrix} \sum_{i=1}^{n}\varphi^2 & \sum_{i=1}^{n}\varphi \\ \sum_{i=1}^{n}\varphi & n \end{vmatrix}},$$

$$c_x = \frac{\Delta c_x}{\Delta} = \frac{\begin{vmatrix} \sum\varphi^2 & \sum_{i=1}^{n} x_i \cdot \widetilde{\varphi} \\ \Delta\varphi \cdot \sum_{i=1}^{n} \varphi & \Delta\varphi \cdot \sum_{i=1}^{n} x_i \end{vmatrix}}{\begin{vmatrix} \sum\varphi^2 & \Delta\varphi \sum_{i=1}^{n} \varphi \\ \Delta\varphi \cdot \sum_{i=1}^{n} \varphi & \Delta\varphi^2 \cdot n \end{vmatrix}} = \frac{1}{\Delta\varphi} \frac{\begin{vmatrix} \sum\varphi^2 & \sum_{i=1}^{n} x_i \cdot \widetilde{\varphi} \\ \sum_{i=1}^{n} \varphi & \sum_{i=1}^{n} x_i \end{vmatrix}}{\begin{vmatrix} \sum\varphi^2 & \sum_{i=1}^{n} \varphi \\ \sum_{i=1}^{n} \varphi & n \end{vmatrix}}.$$

After determination the coefficients c_x, b_x was found

$$a_x = \frac{1}{n} \sum_{i=1}^{n} \left[\frac{x_i}{\varphi_i^{b_x} \exp(c_x \varphi_i)} \right]$$

that is, determined all the coefficients of the empirical dependence (3).

Similarly, we find the coefficients $a_y, b_y, c_y, a_v, b_y, c_y$ of dependences (4) and (5), which allows us to determine the volume.

The analytical description of the numerical solution of the differential equation (1) by the empirical formulas (9-11) can be considered quite accurate [6-7]. Thus, on the basis of the empirical dependences obtained, prototypes of the drop contours are obtained.

To conduct experimental research of the density and surface properties of metallurgical melts, we have developed a facility made of low alloy steel. To obtain an image of a droplet, the installation is equipped with an optical system capable of moving in horizontal and vertical planes. The optical image of the object under research is formed by a Stemi SV 11 horizontal optical microscope and transmitted using an SONY SPT-M308CE monochrome video camera as an analog signal to a DATA TRANSLATION image grabber (frame grabber) (DT-3155). The digitized image with a spatial resolution of 768x576 pixels and 256 levels of gray is placed in the memory of an Intel computer for further processing.

The detection of droplet boundaries was carried out in three stages, according to the method described in works [20-23]. At the first stage, the operator

$$G_x \equiv \frac{\partial f(x,y)}{\partial x} = (f(x+1,y+1) + 2f(x+1,y) + f(x+1,y-1)) -$$
$$-(f(x-1,y+1) + 2f(x-1,y) + f(x-1,y-1)),$$
$$G_y \equiv \frac{\partial f(x,y)}{\partial y} = (f(x+1,y-1) + 2f(x,y+1) + f(x-1,y+1)) -$$
$$-(f(x+1,y-1) + 2f(x,y-1) + f(x-1,y-1))$$

is used in the entire field of the image under research to calculate the gradients in columns and in rows. Pixels with the largest intensity gradient value are selected for further processing. At the second stage, the magnitudes of the intensity gradients for the pixels selected at the first stage are compared in the horizontal, vertical and diagonal directions, and the maximum value is selected. In its direction, an approximation is made by a natural cubic spline under certain boundary conditions

The coordinate of the intersection point of the gray intensity level (half sum of the upper and lower plateaus) and the approximating curve is chosen. At the third stage, using the least squares method for each of five consecutive points along the profile of the lying drop, a second-order polynomial is selected. The pixels of the drop border, which are used for further mathematical processing, are calculated as the midpoint of such a polynomial curve.

5 Experiments and results

Comparison of geometric drops of pure metal melts and those obtained by calculation show their identity, which guarantees the accuracy of the measurements made (Fig. 4).

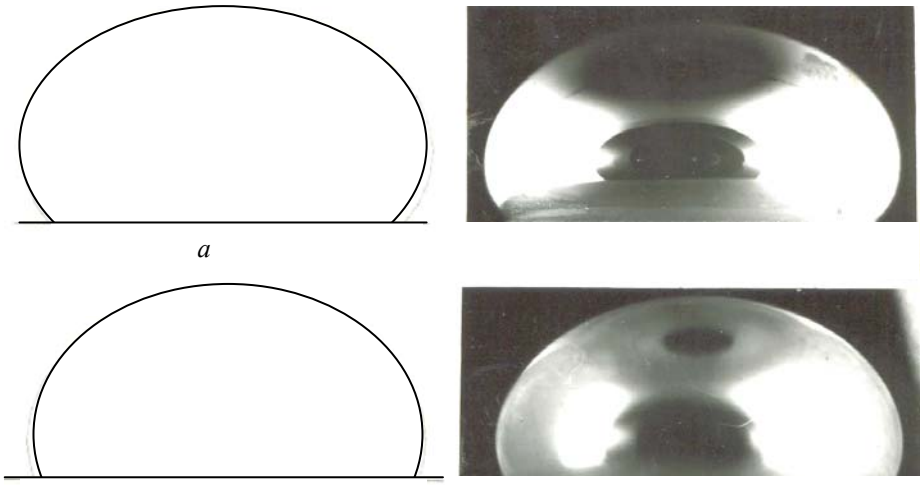

Figure4. Geometrical parameters of melt drops:
а – melt pure iron, at a temperature1600°C;
б – melt pure iron, at a temperature 1500°C.

The study of the wetting angle of the studied slag mixtures on steel 09G2S at 1600 ° C using the proposed method was carried out. The measurement results are shown in Table 1, where by positive experience is meant such that it is possible to clearly define the point of contact and build a tangent line. Accuracy increased by 2-2.5 times.

Table 1. Contact angle of SFM at the interface with steel 09G2S

Slagmixture	The proposed method		Known method		Amount of experiments			
					prototype		The proposed method	
	θ, grade	Measurement error	θ, grade	Measurement error	Total number	Positive experience	Total number	Positive experience
1	54°40′	1%	52°	2,2%	3	1	3	3
2	54°	0,5%	52°	2,6%	4	2	4	3
3	53°20′	0,8%	51º	2,4%	3	2	3	3
4	59°	1,1%	56°	3%	5	2	5	4
5	57°20′	0,9%	55°	2,1%	3	1	3	3
6	54°	0,75%	52°	1,9%	4	1	4	4
7	54°58′	1%	52°	2,7%	3	1	3	2
8	55°	0,5%	55°	2,9%	4	2	4	4
9	55°60′	1,01%	53°	3,1%	5	2	5	4
10	56°36′	0,95%	54°	2,4%	2	1	2	2

6 Conclusion

Techniques for solving the basic equation of a drop surface based on an improved mathematical apparatus with the implementation of Delphi visual programming in the system was improved, which significantly speeds up data processing and fully automates the calculation of the surface tension of melts with a high degree of accuracy (less than 0.5%) compared to known techniques.

A high-temperature experimental facility has been developed for the research of the surface properties of metallurgical melts, which, unlike the known facilities, is equipped with an optical system and a personal computer that allow the digital image of a lying drop, obtained in the experiment, to be processed using a high-speed software package, which significantly reduces the time for experiment and allows to store data and simplifies the work of the experimenter.

References

1. Streinrück, H., Rudische, C.: Numerical investigation of the entrainment of flux into the lubrication gap in continuous casting of steel: Fifth World Congress on Computational Mechanics July 7–12, 2002, Vienna, Austria, 256-271 (2002).
2. Thomas. B. G., Jenkins, M. S., Mahapatra, R. B.: Investigation of strand surface defects using mould instrumentation and modeling. Ironmaking & Steelmaking. Processes, Products and Applications, 18, 485-494(2013). doi.org/10.1179/030192304225019261

3. Maeda, M., Nakamura, N., Takeoka N.: Improvement on Mold Powder for Higher Speed Continuous Casting of Low Carbon Al-killed Steel. Nissin Seiko Giho, 57, 42-53 (1987).
4. Jonayat, A., Thomas, B.G.: Transient thermo-fluid model of meniscus behavior and Slag consumption in steel continuous casting. The Minerals, Metals & Materials Society and ASM International 2014, 45, 1842-1864 (2014). doi: 10.1007/s11663-014-0097-9
5. Irvin, W.R., Perkins, A., Brooks, M.G.: Effect of chemical, operational, and engineering factors on segregation in continuously cast slabs. Iron and Steelmaking. 11, 152-162 (1984).
6. Carlà, M., Cecchini, R.: An automated apparatus for interfacial tension measurements by the sessile drop technique. Review of Scientific Instruments 62, 1088-1097 (1991). doi.org/10.1063/1.1142011
7. Bashforth F., Adams JC.: An attempt to test the theories of capillary action: by comparing the theoretical and measured forms of drops of fluid. Cambridge Univ. Press Cambridge (1883).
8. Smolders, C. A., Duyvis, E. M.: Contact angles; wetting and de-wetting of mercury: Part I. A critical examination of surface tension measurement by the sessile drop method. Recueil des Travaux Chimiques des Pays-Bas. 80(6), 588-680 (1961). doi.org/10.1002/recl.19610800607
9. Girault, H. H.J., Schiffrin, D. J., Smith, B.D.V.: The measurement of interfacial tension of pendant drops using a video image profile digitizer. Jornal of Colloid and Interface Sci. 101(1), 257-266 (1984). doi.org/10.1016/0021-9797(84)90026-2
10. Carla, M., Ceechini, R., Bordi, S.: An automated apparatus for interfacial tension measurements by the sessile drop. Review of Scientific Instruments. 62(4), 1088 -1092 (1991). doi.org/10.1063/1.1142011
11. Goicochea , J., Garcia-Cordovilla C., Louis, E., Pamies, A.: Surface tension of binary and ternary aluminium alloys of the systems Al-Si-Mg and Al-Zn-Mg. Journal of Materials Science. 27(19), 5247-5252 (1992).
12. Liggieri, L., Passerone A.: An automatic technique for measuring the surface tension of liquid metals. High Temperature Technology.7(2), 82-86 (1989). doi.org/10.1080/02619180.1989.11753417
13. Rotenberg, Y., Boruvka, L., Neumann, A. W.: Determination of surface tension and contact angle from the shapes of axisymmetric fluid interfaces. Journal Colloid and Interface Sci. 93(1), 169-183(1993). doi.org/10.1016/0021-9797(83)90396-X.
14. Faour ,G., Grimaldi, M., Richou, J., Bois, A.: Real time pendant drop tension meter using image processing with interfacial area and interfacial tension control capabilities. Journal Colloid and Interface Sci. 181(2), 385-392(1996). doi.org/10.1006/jcis.1996.0395.
15. Hond-Kee, L., Frohberg, G., Martin, P., Haira J.: Surface tension measurements of liquid iron-nickel-sulphur ternary system using the electromagnetic oscillating droplet technique. 1SIJ International. 33(8), 833-838 (1993). doi: 10.2355/isijinternational.33.833
16. Andrien, C., Sykes, C., Brochard, F.: Average speading parameter on heterogeneous surfaces. Langmuir. 10(7), 2077-2080 (1994). doi: 10.1021/la00019a010
17. Emelyanenko, A.M., Boinovich, L.B.: The role of discretization at the video image processing in sessile and pendant drop methods. Colloids and surfaces A: Physicochemical and Engineering Aspects. 189(1), 197-202(2001). doi: 10.1016/S0927-7757(01)00585-4
18. Berry, J., Neeson, M. J., Dagastine, R. R., Chan D. Y.C., Tabor R. F.: Measurement of surface and interfacial tension using pendant drop tensiometry. Journal of Colloid and Interface Science. 454(15), 226-237 (2015). doi: 10.1016/j.jcis.2015.05.012
19. Moser, Z., Gasior, W., Pstrum, J.: Surface tension measurements of the Bi-Sn and Sn-Bi-Ag liguid alloys. Journal of Electronic Materials. Mater. 30(9), 1109-1111(2001).

20. Hansen, F.K., Rodsrud, G.: Surface tension by pendant drop. J.Colloid Interface Sci. l4l (1), 1-9 (1991).
21. Thiessen, D.B, Chione, D.J., McCreary, C.B., Kiantz, W.B. Robust digital image analysis of pendant drop shapes. Journal of Colloid and Interface Science. 177(2), 658-665(1996). doi.org/10.1006/jcis.1996.0080
22. Duncan, D., Li, D., Gaydos, J., Neumann, A.W.: Correlation of line tension and solid-liquid interfacial tension from the measurement of drop size dependence of contact angles. 169(2), 212-217(1995). doi.org/10.1006/jcis.1995.1032
23. Río, O.I., Neumann, A.W.: Contact angle measurements by axisymmetric drop shape analysis and an automated polynomial fit program. Colloids and Surfaces A: Physicochemical and Engineering Aspects. 143(2-3), 197-210 (1998). doi.org/10.1016/S0927-7757(98)00257-X